

# Diffusion of Hydrogen Through Ordered and Disordered Pd-12.5 at% Ce alloys

Yoshiichi SAKAMOTO\* and Yoshizumi TANAKA\*

The diffusivity of hydrogen in ordered and disordered states of Pd-12.5 at% Ce alloys was measured at room temperatures by an electrochemical permeation method. The ordered state has higher diffusivity and low activation energy for diffusion compared with those of the disordered state. The proposed models for the ordered state provide a good description of the experimental results of diffusivity in the alloy. The lower diffusivity of hydrogen in the disordered state can be explained in terms of the trapping effect at the lattice imperfections such as dislocations and the strain fields associated with the dissolved Ce atoms and/or Ce-Ce nearest neighbors.

## 1. Introduction

Recently, the presence of long-range order in a Pd-12.5 at% Ce alloy has been known from electron microscopic observations [1,2] and from measurement of electrical resistance [2]. The stoichiometry of this ordered structure is Pd<sub>7</sub>Ce and it has the structure previously reported for Pt<sub>7</sub>Cu [3].

The influence of the state of order on hydrogen solubility isotherms in the Pd-12.5 at% Ce alloy has been studied [4,5]. The results indicate that the transition from order to disorder in the alloy exhibits an enhanced solubility of hydrogen, which may correspond to the difference in the free energies of hydrogen between the octahedral interstitial sites present in the ordered and disordered structures, or may be attributed to a trapping contribution to the enthalpy associated with the presence of strain fields due to Ce-Ce nearest neighbors.

The anomalies in the temperature dependence of hydrogen diffusivity in some alloys [6-10] with order-disorder transformation have been observed such that there is a sudden change in both the pre-exponential factors for diffusivity and the activation energy for diffusion, or only the activation energy changes. The change in diffusivity of hydrogen with ordering is clearly related to the fact that the potential energies of hydrogen in the interstitial sites and the jump rates between the sites in the migration process should be varied depending on the configuration of the alloying atoms around the sites.

The theoretical study of ordering in some binary alloys on interstitial atom diffusion has been carried out by Krivoglaz and Smirnov [11] on the basis of statistical considerations by assuming that the interstitial atoms in the alloys migrate through two different octahedral-octahedral sites surrounded by different numbers of the two metal atoms, and that the concentration of interstitial atom in the sites is determined by the potential energies of the atoms at the sites and the probabilities of the configuration of the neighboring metal atoms around the individual sites.

Recent reports [12,13] are concerned with an analysis of the diffusion models in fcc solid solution alloys [12] and in some ordered alloys [13]. In the models, hydrogen atoms are assumed to jump through the two types of octahedral and tetrahedral interstitial sites, and the fluxes through the sites have been generally analyzed with classical theory by taking account of the site fraction, the jump fraction, the jump rate between the sites and the gradient of the occupation probability related to the free energies in the individual sites.

The aim of the present work is to examine hydrogen diffusivity in the ordered and disordered Pd-12.5 at% Ce

alloys in the vicinity of room temperature and to discuss the diffusion behavior with the models proposed for the ordered and disordered structures.

## 2. Experimental procedure

The alloy was prepared by arc-melting in argon gas atmosphere from Pd (99.98 wt%) and Ce (99.9 wt%), their planned cerium content being 12.5 at%. The button was inverted and re-melted several times and was subjected to homogenizing anneal at 1123 K for 2 days, and then it was rolled to about 115  $\mu\text{m}$  foils with intermediate anneals when necessary. Finally, the sample was annealed at 1123 K for 2 hrs and then furnace cooled to room temperature to obtain the material in the long-range ordered state. In order to retain disordered state in this alloy, very rapid quenching is necessary and the foils were wrapped in titanium foil and sealed off in evacuated silica tubes and then heated to about 1193 K, after which they were quenched into ice water simultaneously breaking the silica container. The electron microscopic studies were carried out with Hitachi H-800 electron microscope. The samples for the electrical resistance measurements, which were carried out in vacuo were cut into the dimension of about 2 mm x 30 mm from the foils and the conventional four-probe technique was employed using a current of 1 mA.

The diffusivity measurements were carried out by an electrochemical permeation method [14-16]. With the initial and boundary conditions

$$\begin{aligned} t \leq 0 : 0 \leq x \leq L ; C = 0 \\ t > 0 : x = 0 \quad ; C = C_0 \\ \quad \quad \quad x = L \quad ; C = 0 \end{aligned} \quad (1)$$

the rate of permeation (permeation current density)  $J_t = -FD [\partial C(x,t) / \partial x]_{x=L}$ , as the function of time is given as

$$J_t = \frac{2\sqrt{D} C_0 F}{\sqrt{\pi t}} \sum_{n=0}^{\infty} \exp\left[-\frac{(2n+1)^2 L^2}{4Dt}\right] \quad (2)$$

where  $D$  = diffusivity of hydrogen,  $C_0$  = concentration of hydrogen beneath the cathodic surface,  $L$  = thickness of specimen,  $F$  = Faraday's constant,  $t$  = permeation time. The diffusivity was determined from the build-up transient of the permeation curve by using the linear relation of  $\log(\sqrt{t}J_t)$  vs.  $1/t$  which is the first term ( $n = 0$ ) of eq. (2). The experimental apparatus and the procedures for measuring the rate of hydrogen permeation under the galvanostatic charging conditions were similar to those described previously [15,16]. All the samples were chemically polished in 2 vol : 2 vol : 1 vol of  $\text{H}_2\text{SO}_4$  :  $\text{HNO}_3$  :  $\text{H}_2\text{O}$  mixture prior to the permeation measurements. The anodic compartment of the permeation cell was filled with  $0.1 \text{ k mol m}^{-3}$  NaOH solution and an anodic potential of  $-175\text{mV}$  vs. Ag/AgCl reference electrode was applied at the diffusion side of the specimen using a potentiostat. The specimen was cathodically polarized at a constant current density  $i_c = 10 \text{ Am}^{-2}$  in the cathodic compartment which contained a solution of  $160 \text{ mol m}^{-3}$   $\text{H}_2\text{SO}_4$  and  $2.5 \times 10^{-3} \text{ kg m}^{-3}$   $\text{H}_2\text{SeO}_3$ . The cell was enclosed in a thermostatic air bath that was controlled at the temperature within  $\pm 1 \text{ K}$  between 279 and 335 K.

## 3. Diffusion models

We consider the diffusion models of hydrogen in both the disordered and ordered alloys along the  $\langle 110 \rangle$  direction, in which the lines of flow are parallel to the  $x$ -axis. It is assumed that for simplicity, hydrogen atoms occupy octahedral site only, although the previous reports [12,13] have taken account of the diffusion paths through the two types of O and T-interstitial sites.

### 3.1 Disordered lattice

Although two possible migration paths in the  $\langle 110 \rangle$  direction are considered [12] depending on the location of the solute atom, we consider only one of the model paths here, because the other path has too many unknown parameters to enable a comparison to be made of the experimental data.

Figure 1 shows the model path of the migration of hydrogen for the disordered alloy containing randomly substitutional atom. The influence of the lattice defects such as vacancies and dislocations on the diffusion is not consi-

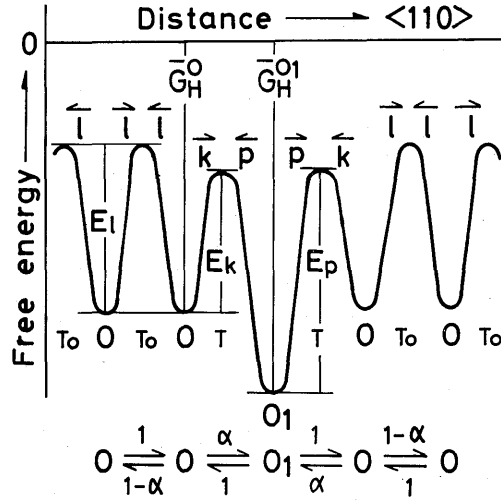


Fig. 1. Energy steps for hydrogen diffusion in the disordered structure.

dered here. It consists of  $O_1$  and  $O$ -sites. The  $O_1$ -site is the 1st nearest neighboring octahedral site around a Ce atom, i. e., it is surrounded by one Ce and five Pd atoms. The  $O$ -site is unaffected by the solute atom. Thus, the site fractions are  $f_o + f_{o_1} = 1$ . The positions of  $T_o$  and  $T$  are assumed to be the saddle points in this model, although the former has two tetrahedral sites which are consisted of only four Pd atoms, and the latter has also two tetrahedral sites where one tetrahedral site is consisted of one Ce atom and three Pd atoms and the other is consisted of only four Pd atoms.  $\bar{G}_H^o$  and  $\bar{G}_H^{o_1}$  are the free energies of hydrogen, for which we choose to measure these energies with respect to the energy of a hydrogen atom at rest in a vacuum. The hydrogen jump rates  $l$ ,  $k$  and  $p$ , the diffusivities  $D_l$ ,  $D_k$ ,  $D_p$ , and the corresponding activation energies  $E_l$ ,  $E_k$ ,  $E_p$ , for diffusion express those for the jumping processes of  $O \leftrightarrow O$ ,  $O \rightarrow O_1$  and  $O \leftarrow O_1$  intersites, respectively.  $\alpha$  is the jump fraction [12] for hydrogen atom at a  $O$ -site to jump to a  $O_1$ -site with the jump rate  $k$ , and  $1 - \alpha$  the jump fraction for hydrogen atom at a  $O$ -site to jump to an adjacent  $O$ -site with the rate  $l$ .

Since the jump with the jump rate  $k$  is the same as that with the jump rate  $p$ , the following relation holds.

$$\alpha f_o = f_{o_1} \quad (3)$$

From the geometry of jump path, we can specify each jump fraction with the value of  $f_{o_1}$ . So that

$$\alpha = f_{o_1}/(1 - f_{o_1}), \quad 1 - \alpha = (1 - 2f_{o_1})/(1 - f_{o_1}). \quad (4)$$

Furthermore, the site fractions of neighboring site around the Ce atom can be given by

$$f_{o_1} = \frac{Z_{o_1} \cdot \theta_u}{\beta_o}, \quad (5)$$

where  $Z_{o_1}$  = the number of the 1st nearest neighboring octahedral sites along the  $\langle 110 \rangle$  direction around the Ce atom, i. e.,  $Z_{o_1} = 2$ .  $\theta_u$  = the foreign metal atom ratio to total metal atom i. e., the atom fraction.  $\beta_o$  = the usual meanings,  $\beta_o = 1$ . Thus, we can obtain  $f_{o_1} = 2\theta_u$  and the effective range of  $\theta_u$  for this model is limited to  $0 < \theta_u < 1/4$ , because  $0 < f_{o_1} < 1/2$ .

When a large number of such migration paths are randomly distributed in the  $x$ -direction, a fiducial plane between  $x$  and  $(x + a)$  planes ( $a$  = unit jump distance) intersects any part of the fluxes across the plane. Therefore, by summing the parts of the fluxes in one lattice plane on the basis of the assumption that there is no interaction among the individual fluxes, we can calculate the total flux corresponding to the situation of migration path illustrated in Fig. 1. All the possible fluxes between the sites due to the gradient of the occupation probability can be obtained [12]. As the total diffusivity  $D$  through the migration path is concerned with the relation between the total flux,  $J_{\text{total}}$  and the gradient of the total hydrogen concentration  $[C_{\text{total}}]$ , i. e.,  $J_{\text{total}} = J_{O \rightarrow O} + J_{O \rightarrow O_1} = -D \partial [C_{\text{total}}] / \partial x$ , where  $[C_{\text{total}}] = f_o C_o + f_{o_1} C_{o_1}$ , we can express the diffusivity in this model by assuming a system of low occupation probability on individual sites, and of the existence of local thermodynamic equilibrium between the sites. So that

$$D = \frac{(1-4\theta_u)D_i^0 \exp\left[-\frac{E_i}{RT}\right] + 2\theta_u(D_k^0 + D_p^0) \exp\left[-\frac{E_k}{RT}\right]}{1 - 2\theta_u \left[1 - \exp\left[-\frac{\Delta\bar{G}_H^{O_1,0}}{RT}\right]\right]} \quad (6)$$

where  $D_i^0$ ,  $D_k^0$  and  $D_p^0$  are the jump frequency factors corresponding to the appropriate  $D$  values.  $\Delta\bar{G}_H^{O_1,0}$  is the free energy change of hydrogen at an  $O_1$ -site with respect to a O-site. Assuming that  $\Delta\bar{S}_H^{xs,O_1,0} = \bar{S}_H^{xs,O_1} - \bar{S}_H^{xs,0} = 0$ , where  $\bar{S}_H^{xs}$  is the excess entropy, the  $\Delta\bar{G}_H^{O_1,0}$  is equal to the difference in partial molar enthalpies of hydrogen between the  $O_1$  and O-site, i. e., the interaction energy of hydrogen. Then, the following relation holds,

$$\Delta\bar{G}_H^{O_1,0} = E_k - E_p \quad (7)$$

As a verification of eq. (6), if  $\theta_u = 0$ , equation (6) reduces to an Arrhenius relation.

### 3.2 Long-range ordered lattice

In the superlattice structure of Pd<sub>7</sub>Ce, two possible migration paths are also considered [13]. The influence of the lattice defects such as the anti-phase domain boundaries, vacancies and dislocations on the diffusion and also the effect of degree of ordering are not considered here.

We first consider the model path shown in Fig. 2- I). The O-site is surrounded by only six Pd atoms and  $O_1$ -site is surrounded by one Ce and five Pd atoms. The site fractions are  $f_o + f_{o_1} = 1$ . The T position is the saddle point.  $\bar{G}_H^O$  and  $\bar{G}_H^{O_1}$  are the free energies of hydrogen at O and  $O_1$ -sites.  $k_1$  is the jump rate from O to  $O_1$ -sites,  $p_1$  the jump rate from  $O_1$  to O-sites. The corresponding activation energies for these jumps are  $E_{k_1}$  and  $E_{p_1}$ , respectively. From the constraint of the jump path, we get  $f_o = 1/2$  and  $f_{o_1} = 1/2$ , although the values of  $f_o$  and  $f_{o_1}$  under the real situation of the lattice are 1/4 and 3/4, respectively.

The diffusivity expression can be given as eq. (8) according to the similar way described in 3.1.

$$D = \frac{D_k^0 \exp\left[-\frac{E_{k_1}}{RT}\right] + D_p^0 \exp\left[-\frac{E_{p_1}}{RT}\right]}{1 + \exp\left[-\frac{\Delta\bar{G}_H^{O_1,0}}{RT}\right]} \quad (8)$$

where  $D_k^0$  and  $D_p^0$  are the jump frequency factors and the energy relation is

$$\Delta\bar{G}_H^{O_1,0} = E_{k_1} - E_{p_1} \quad (9)$$

As a check of eq. (8), if  $\Delta\bar{G}_H^{O_1,0} = 0$  and  $D_k^0 = D_p^0$ , it leads to an Arrhenius relation.

Another migration path in this structure is given in Fig. 2- II). All the  $O_1$ -sites are surrounded by one Ce and five Pd atoms. The saddle point of  $T_o$  has two tetrahedral sites, which are consisted of only four Pd atoms and the  $T_1$  saddle point has also two tetrahedral sites which are consisted of one Ce atom and three Pd atoms. Assuming that

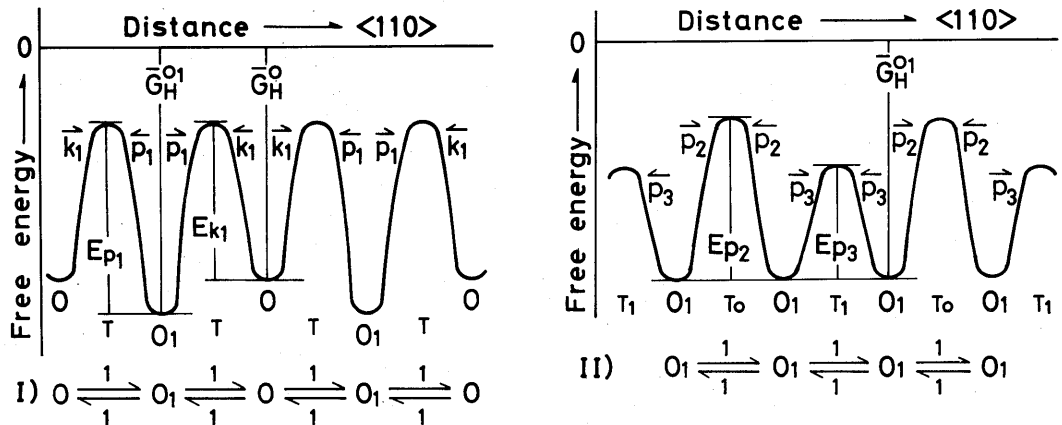


Fig. 2 Energy steps for hydrogen diffusion in the ordered structure.

I) Model-Part I) , II) Model-Part II).

the occupation probability at individual sites is also low, and that the local thermodynamic equilibrium exists between the sites, we can obtain the diffusivity expression. That is,

$$D = \frac{1}{2} \left\{ D_{p_2}^0 \exp \left[ -\frac{E_{p_2}}{RT} \right] + D_{p_3}^0 \exp \left[ -\frac{E_{p_3}}{RT} \right] \right\} \quad (10)$$

where if  $E_{p_2} = E_{p_3}$  and  $D_{p_2}^0 = D_{p_3}^0$ , the expression reduces to an Arrhenius relation. In the actual situation of hydrogen diffusion in this lattice structure, we can regard that the two migration paths shown in Fig. 2- I ) and 2- II ) exists at the same time accompanying with a given flux ratio, respectively.

#### 4. Results and Discussion

##### 4.1 Electron microscopic observations and electrical resistance measurements

The [001] electron diffraction patterns observed for both slowly cooled and rapidly quenched Pd-12.5 at% Ce alloys used in this study are shown in Photos. 1-a) and 1-b), respectively. The structure of the slowly cooled sample was identified as that of Pd<sub>7</sub>Ce proposed previously [1,2], which has superlattice reflections at  $hkl = 100, 1/2 1/2 1/2$  and the equivalents in a cubic reciprocal lattice space. On the other hand, we can see that the electron diffraction pattern of the quenched specimen has no clear existence of the superlattice, but exhibits a weak splitting of spot.

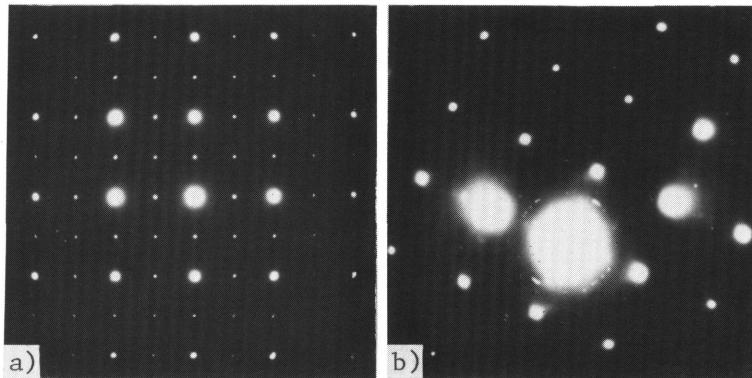


Photo. 1 Electron diffraction patterns of Pd-12.5 at% Ce alloy.  
Beam along [001]  
a) ordered state. b) disordered state.

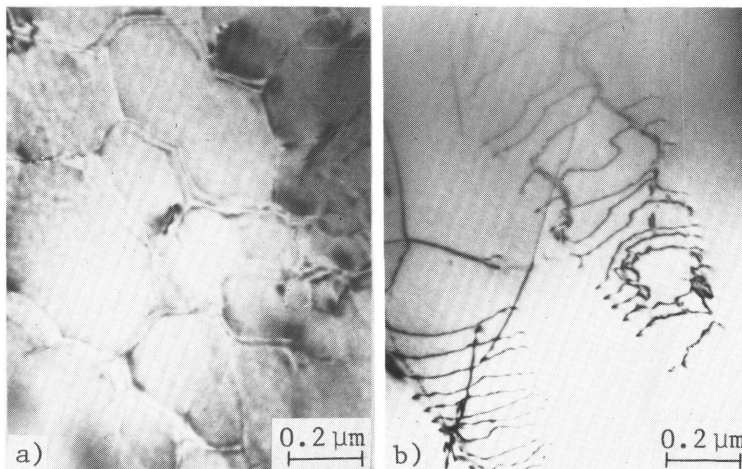
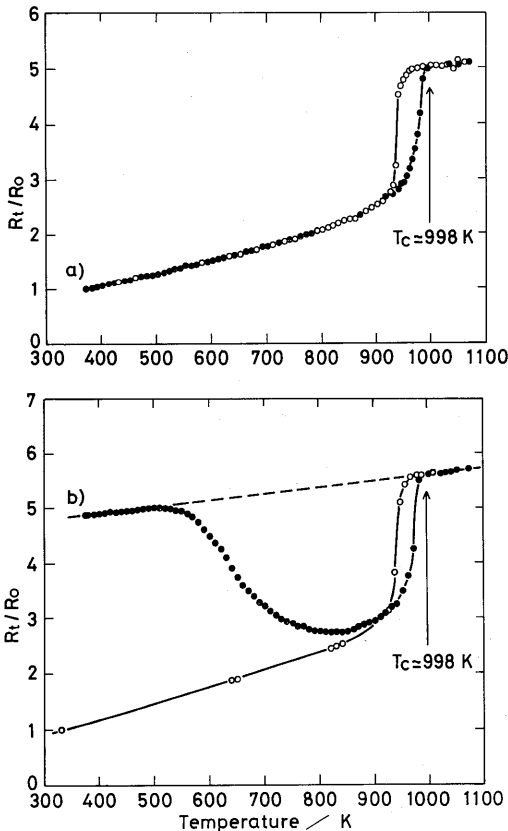


Photo. 2 Bright-field electron micrographs of Pd-12.5 at% Ce alloy.  
a) ordered state. b) disordered state.

As Kuwano et al [1] and Smith et al [4] reported the similar results, it seems that the spot splitting is attributed to the short-range order in the quenched specimen. Photos. 2-a) and 2-b) show the TEM for both the ordered and disordered specimens, respectively. The net-like structure in the ordered sample corresponds to the anti-phase domain boundaries and the quenched sample shows the asymmetrically extended nodes and/or the planer slip of dislocations. Furthermore, X-ray diffraction has been employed to measure the lattice parameters of both samples. The lattice parameter of the ordered alloy Pd<sub>7</sub>Ce was  $a_o = 0.3985 \pm 0.0001$  nm and that of the disordered alloy was  $a_o = 0.3991 \pm 0.0001$  nm. This is consistent with the fact [17,18] that in general, an alloy with a high degree of order has a lower lattice parameter than that in the disordered condition.

The electrical resistance measurements for both alloys were carried out in vacuo by heating and cooling rate of  $2 \text{ K min}^{-1}$ . Figure 3-a) shows the electrical resistance of the alloy which was initially in an ordered state at room temperature and it can be seen that it undergoes a remarkable increase in resistance starting at about 940K leading to a completely disordered state at  $T_c \approx 998$  K. The re-ordering of this alloy can be seen during cooling where there is seen to be a small hysteresis. Figure 3-b) also shows the heating and subsequent cooling curves for the quenched sample. The ordering is seen to commence at about 540 K and the alloy starts to disorder at about 850 K and also finishes at about  $T_c \approx 998$  K. The cooling curve follows the behavior of the initially ordered alloy. Since the low temperature resistance of the quenched alloy extrapolates linearly to coincide the high temperature resistance-temperature behavior of the disordered alloy, it seems reasonable to assume that the quenched alloy is almost in disordered state.



a) initially in the ordered state at room temperature.  
 b) initially in the disordered state at room temperature.

Fig. 3 Electrical resistance-temperature behavior.

● : Heating, ○ : Cooling ; the rate =  $2 \text{ Kmin}^{-1}$ .

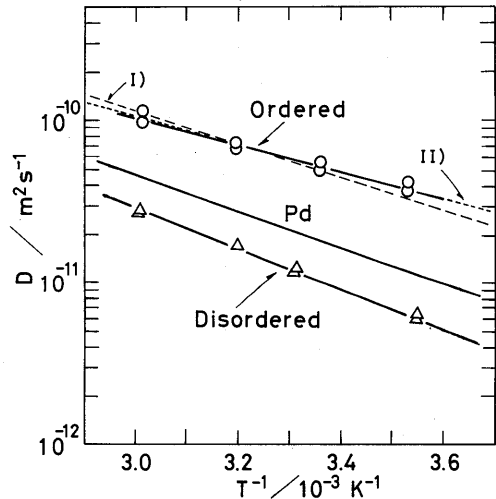


Fig. 4 Temperature dependence of hydrogen diffusivity in the ordered and disordered Pd-12.5 at % Ce alloys.

○ : ordered state, --- Model-Part I),  
 ..... ; Model-Part II) .  
 △ : disordered state.

## 4. 2 Diffusivity of hydrogen

The results of hydrogen diffusivity for both the ordered and disordered alloys are given in Fig. 4, together with that of pure Pd [15] for comparison. The values of the pre-exponential factor  $D^0$  and the activation energy for diffusion were determined by regression analysis and they are summarized in Table 1.

Table 1 Temperature dependence of the diffusivity for the ordered and disordered Pd-12.5 at% Ce alloy in the range of 279-335 K, where  $D = D^0 \exp[-\Delta H_D/RT]$

	$D^0/m_2 s^{-1}$	$\Delta H_D/kJ mol^{-1}$
Ordered	$2.98 \times 10^{-8}$	$15.76 \pm 0.85$
Disordered	$1.89 \times 10^{-7}$	$24.33 \pm 1.24$
Annealed pure Pd	$1.05 \times 10^{-7}$	$21.42 \pm 1.21$

The value of  $D = 1.85 \times 10^{-11} m^2 s^{-1}$  at 298 K in annealed pure Pd is in good agreement with those measured by Devanathan-Stachurski [19], Stackelberg-Ludwig [20] and Hasegawa-Nakajima [21], using the similar electrochemical permeation technique, although the diffusivity values which were determined by the step-method [22] or the pulse-method [23], as well as the other measuring methods [24] such as gas volumetric, Gorsky effect, nuclear magnetic resonance etc., are higher about two times than the present value.

The ordered sample has higher diffusivity and low activation energy for diffusion, compared with those of the disordered sample over the same temperature range. The behaviors of the diffusivity and activation energy for diffusion in the ordered and disordered alloys are in agreement with those of Pd-5.75 at% Ce alloy reported previously [25], although we have not confirmed the existence of any ordering in the alloys of low Ce contents by the electrical resistance measurement between heating and cooling processes and by the electron microscopic study [5]. The lower diffusivity of hydrogen in the disordered state may be explained in terms of the trapping effect at the lattice imperfections such as dislocations and the strain fields associated with the dissolved Ce atoms and/or Ce-Ce nearest neighbors which are discussed by Smith et al [4] in the quenched alloy. In fact, as can be seen from Photo. 2-b), the microstructures show appreciably dislocations. On the other hand, however in the case of the low Ce alloys up to about 7 at%, we have observed the fact by the same measuring method that the diffusivity increases progressively with increasing Ce content and thus the Ce atoms act as the "anti-trapping" effect in the alloys [26]. Therefore, the effect of alloying of Ce atom on the diffusion seems to be different between the low and high Ce alloys, and so we cannot apply the model of eq. (6) derived in 3.1 to the interpretation of experimental data of the disordered state of Pd-12.5 at% Ce alloy.

The ordered structure may be attributed to the lowering of the lattice strain energy associated with large differences in atomic size and electronegativity as compared to the disordered structure, and the effect of anti-phase domain boundary on hydrogen diffusion seems to be little. Assuming that the Arrhenius type relation of diffusivity holds in a wide range of temperature, the linear variations of  $\log D$  vs.  $1/T$  for both specimens intersect at or close to the disorder to re-order transformation temperature of about 540 K for the quenched sample.

Now, we will compare the present models, i. e., eqs. (8) and (10) with the experimental diffusivity data in the ordered state. In comparing the model- I) of the ordered alloy given in Fig. 2- I), i. e., eq. (8) with the experimental data, we assumed that for convenience the values of  $D_{p1}^0$  and  $E_{p1}$  are equal to those of  $D_p^0$  and  $E_l$  for pure Pd [15], respectively. By taking  $D_{p1}^0$  and  $E_{p1}$  as unknown parameters, the sum of the squared errors was calculated as a function of temperature. This process was iterated for a wide range of  $D_{p1}^0$  and  $E_{p1}$  values until a minimum in the sum of the squared errors was found, where the energy was stepped in intervals of 0.1 kJ mol<sup>-1</sup>. The best fit values were found to be  $D_{p1}^0 = 2.3 \times 10^{-7} m^2 s^{-1}$  and  $E_{p1} = 17.5 kJ mol^{-1}$ . On the other hand, in fitting eq. (10) of mod-

el- II) for the ordered alloy with the observed data, we assumed that both values of  $E_{p_2}$  and  $E_{p_3}$  are also the same to  $E_{p_1}$  obtained above. The best fit value of  $(D_{p_2}^0 + D_{p_3}^0)$  was  $1.2 \times 10^{-7} \text{ m}^2 \text{ s}^{-1}$ . The calculated results are shown in Fig. 4 with the dotted lines. Despite the degree of simplification involved, the present models provide a good description of the experimental data for the ordered alloy.

The schematic energy profiles for the diffusion are shown in Fig.5 together with the activation energy and the jump frequency factors obtained from the best fit. Although the  $T_0$  and  $T_1$ -positions in the model- II) of the ordered alloy shown in Fig. 2- II) are assumed to be the saddle point, the former has two tetrahedral sites which are consisted of only Pd atoms and the latter has also two tetrahedral sites which are consisted of one Ce atom and three Pd atoms. So, both the jump frequency factors  $D_{p_2}^0$  and  $D_{p_3}^0$  are not equal, however at this stage we cannot distinguish the difference between them. As described before, in the actual situation of the diffusion process in the alloy, it is considered that the hydrogen fluxes occur simultaneously with a given flux ratio through the two migration paths.

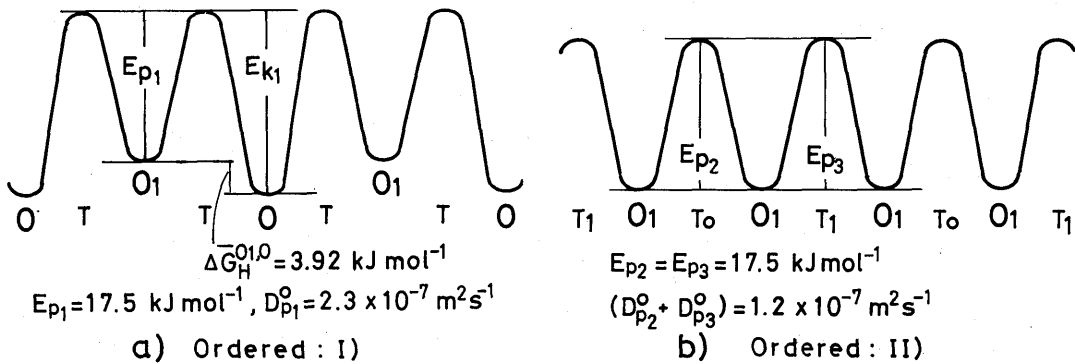


Fig. 5 Calculated energy steps and frequency factors for the diffusion models of the ordered state.

- a) Model-Part I).
- b) Model-Part II).

## 5. Conclusions

The results of this study can be summarized as follows:

The presence of long-range order of Pd<sub>7</sub>Ce structure in slowly cooled Pd-12.5 at% Ce alloy was confirmed by electron microscopic observations and from measurements of electrical resistance, the critical temperature of the order-disorder transformation in the alloy was found to be  $T_c = 998 \pm 5 \text{ K}$ . The rapidly quenched alloy was almost in disordered state.

The ordered state has higher hydrogen diffusivity and low activation energy for diffusion compared with those of the disordered state. The proposed diffusion models for the ordered alloy provide a good description of the experimental data. The lower diffusivity of hydrogen in the disordered state can be explained in terms of the trapping effect at the lattice imperfections such as dislocations and the strain fields associated with the dissolved Ce atoms and/or Ce-Ce nearest neighbors. Thus, the model eq. (6) derived in this study cannot interpret the experimental data of hydrogen diffusivity in the disordered state.

## References

1. N.Kuwano, T.Shiwaku, Y.Tomokiyo and T.Eguchi : Jpn. J. Appl. Phys., **20** (1981) , 1603.
2. D.A.Smith, I.P.Jones and I.R.Harris : J.Mater. Sci. Letters, **1** (1982) , 463.
3. A.Schneider and U.Esch : Z. Elektrochem., **50** (1944) , 290.
4. D.A.Smith, I.P.Jones and I.R.Harris : J. Less-Comm. Met., **103** (1984) , 33.
5. Y.Sakamoto, T.B.Flanagan and T.Kuji : Z. Phys. Chem., N.F., **143** (1985) , 61.
6. R.Dus and M.Smialowski : Acta Met., **15** (1967) , 1611



7. V.A.Gol'tsov, V.B.Vykhodets, P.V.Gel'd and Yu.P.Simakov : Fiziko-Khim.Mekh. Mat., **5** (1969) , 597.
8. V.B.Vykhodets, V.A.Gol'tsov and P.V.Gel'd : Ugr. Fiz. Zh., **5** (1970) , 107.
9. V.B.Vykhodets, V.A.Gol'tsov and P.V.Gel'd : Fiz. metal metalloved., **26** (1968) , 933.
10. G.P.Smirnova and L.L.Kunin : Fiz. metal metalloved., **23** (1967) , 737.
11. M.A.Krivoglaz and A.Smirnov : "The Theory of Order-Disorder in Alloys", Macdonald & Co., Ltd., London (1964).
12. Y.Sakamoto : "Proceedings of the 30 th Japan Congress on Materials Research", The Soc. of Materials Sci., Japan, in press.
13. Y.Sakamoto and K.Baba : *ibid.*
14. J.McBreen, L.Nanis and W.Beck : J. Electrochem. Soc., **113** (1966) , 1218.
15. Y.Sakamoto and N.Tabaru : J. Jpn. Inst. Met., **45** (1981) , 1048.
16. Y.Sakamoto and T.Nishino: "Proc. 24 th Japan Congress on Materials Research" , P. 178 (1981), The Soc. of Materials Sci., Japan.
17. A.J.Bradley and A.H.Jay : J. Iron Steel Inst., **125** (1932) , 339.
18. A.Taylor and K.G.Hinton : J. Inst. Met., **81** (1952-1953) , 169.
19. M.A.V.Devanathan and Z.Stachurski : Proc. Roy. Soc., **A270** (1962) , 90.
20. M.v.Stackelberg and P.Ludwing : Z.Naturforsch., **19a** (1964) , 93.
21. H.Hasegawa and K.Nakajima : J. Phys., F, **9** (1979) , 1035.
22. H.Züchner and N.Boes : Ber. Bunsenges. Physik. Chem., **76** (1972) , 783.
23. H.Züchner : Z. Naturforsch., **25a** (1970) , 1490.
24. J.Völkl and G.Alefeld : "Hydrogen in Metals I" , p. 324 (1978) , Springer-Verlag, Berlin.
25. D.T.Hughes, J.Evams and I.R.Harris : J. Less-Comm. Met., **74** (1980) , 255.
26. Y.Sakamoto, H.Kaneko, T.Tsukahara and S.Hirata : "Collected Abstracts in 1984 Spring Meeting of JIM", Tokyo (1984) , p. 201.